DIGITAL ACCESS TO SCHOLARSHIP AT HARVARD
DASH.HARVARD.EDU

HARVARD LIBRARY
Office for Scholarly Communication

Standard Chemoradiation for Glioblastoma Results in Progressive Brain Volume Loss

Citation

Prust, Morgan. 2015. Standard Chemoradiation for Glioblastoma Results in Progressive Brain Volume Loss. Doctoral dissertation, Harvard Medical School.

Permanent link

http://nrs.harvard.edu/urn-3:HUL.InstRepos:17295906

Terms of Use

This article was downloaded from Harvard University's DASH repository, and is made available under the terms and conditions applicable to Other Posted Material, as set forth at http://nrs.harvard.edu/urn-3:HUL.InstRepos:dash.current.terms-of-use#LAA

Share Your Story

The Harvard community has made this article openly available.
Please share how this access benefits you. Submit a story .

Accessibility

Table of Contents

Acknowledgements

This project was a collaboration between neuro-oncologists, neuroimaging experts, and myself (the specific roles and contributions of each collaborator are outlined on the following page). First and foremost, I would like to sincerely thank my mentor, Dr. Jorg Dietrich, a neuro-oncologist and stem cell biologist at Massachusetts General Hospital. He has supported my research since my first semester of medical school, and his expertise, guidance and generosity of time and energy have made our collaboration a productive and truly enjoyable one.

I would also like to thank each of my colleagues who have contributed to this work in various ways and who are listed as co-authors on a manuscript of this work that we have submitted for publication. This group includes Drs. Khourosh Jafari-Khouzani, Jayashree Kalpathy-Cramer and Pavlina Polaskova, all imaging scientists at the MGH-affiliated Martinos Center for Biomedical Imaging. All of them devoted significant time not only the data processing and analysis included in this report, but to helping me learn many of the technical aspects of image processing. This group also includes Dr. Elizabeth Gerstner, a neuro-oncologist and investigator in cancer neuroimaging at both MGH and the Martinos Center. Without Elizabeth's expertise in both of these areas, this project would not have been possible. Finally, I would like to thank Dr. Tracy Batchelor, director of the Stephen E. and Catherine Pappas Center for Neuro-Oncology at MGH, who contributed to the design and interpretation of our study.

This research would not have been possible without the Harvard Medical School Scholars in Medicine Program, which helped me find my current lab and supported me during a summer of concentrated research time. I am particularly grateful to Dr. Gordon Strewler, my thesis advisor, who helped me develop my approach to this project and has been a source of guidance and support throughout my time at HMS.

Above all, I would like to thank the patients who participated in this study. Each of them submitted to a long and extensive protocol of serial neuroimaging while enduring the burdens of their disease and the treatments that are needed to treat it. This contribution is selfless and invaluable.

Collaborator contributions

I designed the present study in close collaboration with Jorg Dietrich and Elizabeth Gerstner. With technical assistance from Khourosh Jarafi-Khouzani, Jayashree Kalpathy-Cramer and Pavlina Polaskova, I conducted the image processing and data analysis. I wrote the manuscript, with editing contributions from Jorg Dietrich, Elizabeth Gerstner and Tracy Batchelor.

Glossary of abbreviations and terms

ADC: apparent diffusion coefficient, measured on diffusion tensor imaging.
Chemoradiation: the concurrent administration of systemic chemotherapy and radiation therapy
DTI: diffusion tensor imaging, a neuroimaging modality used to assess properties of the brain's white matter through measurement of free water diffusion in tissue.
FA: fractional anisotropy, measured on diffusion tensor imaging.
GM: grey matter
MRI: magnetic resonance imaging
NPC: neural progenitor cell
RT: radiation therapy
SVZ: subventricular zone, a cell-dense region adjacent to the ependyma which contains a high density of neural progenitor cells
WM: white matter

Introduction

With the increasing success of anti-cancer therapies, treatment-associated sequelae among survivors have emerged as an important and challenging clinical issue. Neurocognitive impairment following systemic chemotherapy has gained particular attention, with published studies, predominantly from patients treated for breast cancer, reporting subjective symptoms and measurable cognitive deficits ranging from 17-75% of patients (Van Dam et al., 1998; Schagen et al. 1999; Ahles et al., 2002; Wefel et al., 2004). Effects have been observed in an array of cognitive domains, including working memory, attention, executive function, visuospatial reasoning and psychomotor reaction time (Correa et al., 2012). Patients with CNS malignancy appear to be at particular risk for neurotoxic side effects, given the combined effects of chemotherapy and cranial irradiation, which comprise the standard of care for several types of brain cancer (Taphoorn & Klein, 2004; Dietrich et al., 2008; Tanaka et al., 2013). Treatment-associated neurotoxicity and its cognitive sequelae prevent many patients from returning to pre-treatment functional status in their professional and personal lives.

This scholarly project aims to explore whether structural changes in healthy human brain tissue during exposure to chemotherapy and cranial irradiation can be detected with in vivo neuroimaging (here, "healthy" is meant to denote brain tissue that is radiographically unaffected by tumor). To the extent that such changes can be detected, it aims to characterize their distribution, magnitude and time course. Interest in this area is rooted in the need for accessible biomarkers of neurotoxic injury. A precise view of how healthy brain structures change through exposure to chemical and radiation toxicity is important, as it would allow us to visualize and how ongoing neurotoxic exposure changes healthy tissue over time. Understanding these changes sets the stage for future investigations into the relationship between measured brain

changes and discreet measures of neurocognitive performance, and whether individual differences in long-term neurologic outcomes may be predicted by neuroimaging.

By way of introduction, we will review preclinical models of neurotoxicity from systemic chemotherapy and cranial irradiation. We will then review the burgeoning body of human neuroimaging studies in this area. The introduction will conclude with a description of the present study's design.

Neural progenitor cells, neurogenesis and proposed mechanisms of treatment-associated toxicity

Much of the work in preclinical models of treatment-associated neurotoxicity supports the involvement of neural progenitor cells (NPCs), which appear particularly vulnerable to neurotoxic injury (Monje et al., 2002; Dietrich et al., 2006; Han et al., 2008; Dietrich et al., 2008) are integral in maintaining, remodeling and replenishing the structure and connectivity of the CNS across the lifespan (Eriksson et al., 1998; Zhao et al., 2008; Deng et al., 2010). NPCs encompass neural stem cells (NSCs), neuron-restricted precursor cells (NRPs) involved in neurogenesis, and glial-restricted precursor cells (GRPs).

NPCs are found in discreet cellular pools located in the hippocampus, subjacent to the ventricles, and throughout the subcortical white matter of the brain (Chang et al., 2000; Zhao et al., 2008; Monje & Dietrich, 2012). NSCs in the dentate gyrus of the hippocampus drive hippocampal neurogenesis, a process believed to underlie a wide array of cognitive functions including episodic memory, executive cognition, cognitive processing speed and attention (Zhao et al., 2008; Deng et al., 2010). According to the neurogenic reserve hypothesis (Kempermann, 2008), NSCs supply the hippocampus with a pool of highly plastic cells, which mature into neurons on an ongoing basis and become integrated into the hippocampal formation to

strengthen and expand networks essential for neurocognitive function. Hippocampal neurogenesis is increased in mice following exercise (van Praag et al., 1999) and in those reared in enriched sensory environments (Kempermann et al., 1997). Furthermore, diminution of hippocampal neurogenesis in mice decreases performance on the hippocampus-dependent Morris Water Maze (Lemaire et al., 2000). It is plausible that the delayed cognitive deficits seen in cancer patients treated with chemotherapy and/or radiation may arise from injury to the progenitor cell pool, with diminished neurogenic potential in the hippocampus failing to meet the brain's neurocognitive demands.

Beyond the hippocampus, NPCs are densely concentrated in the subventricular zone (SVZ), which lies adjacent to the ependyma, a thin cellular layer lining the lateral ventricles of the brain. It is among the most cellularly dynamic and vessel-rich territories within the CNS and is replete with slowly and rapidly dividing cells important for neurogenesis and endogenous CNS repair. SVZ progenitor cells have been shown to contribute to neurogenesis in the olfactory bulb, migrating anteriorly from the SVZ via a path known as the rostral migratory stream (Curtis et al., 2007; Zhao et al., 2008). The full range of functions of SVZ progenitor cells and their precise contributions to neurogenesis are incompletely understood. Finally, oligodendrocyte precursor cells (OPCs) are found throughout the subcortical white matter and give rise to oligodendrocytes, which myelinate the subcortical white matter during the first two decades of life (Chang et al., 2000).

Chemotherapy and radiation appear to injure CNS tissue through independent mechanisms. Many classes of chemotherapeutic agents have been shown to directly target normal brain cells, with self-renewing NPCs and oligodendrocytes among the most vulnerable to neurotoxic insult (Dietrich et al., 2006). In animal models, exposure to a variety of

chemotherapeutic agents is associated with dose-dependent cell death and suppression of cellular proliferation in brain regions critical to brain plasticity, gliogenesis and neurogenesis, including the hippocampal dentate gyrus and the lateral subventricular zone (Dietrich et al., 2006; Monje & Dietrich, 2012). *In vitro* analyses suggest that these cellular phenotypes occur immediately after exposure, but that widespread effects on brain structure and function, including damage to WM tracts, may be at least partially governed by a delayed neurotoxic process (Han et al., 2008). Collectively, preclinical studies suggest that chemotherapy injures CNS tissue through a combination of short- and long term effects related to direct cytotoxicity and depletion of NPC and glial cells, leading in turn to impaired neurogenesis and maintenance of WM integrity.

Radiation-induced CNS injury is traditionally defined as acute (onset within days of exposure), early delayed (onset within 1-6 months) and late delayed (onset after months to years; Tofilon and Fike, 2000; Correa, 2007). Late delayed injury affects neural and vascular endothelial progenitor cells, and is associated with progressive and potentially irreversible changes in brain anatomy and cognitive function. Like chemotherapy, brain RT has also been shown to increase neural progenitor cell apoptosis and to decrease cell proliferation in regions important for ongoing neurogenesis throughout the adult lifespan (Tada et al., 2000; Monje et al., 2002). Radiation also accelerates hippocampal cell death (Peissner et al., 1999), and long term decreases in the number, density and complexity of dendritic spines in the hippocampal dentate gyrus has been observed following radiation exposure in a mouse model (Parihar & Limoli, 2013).

While work is ongoing to elucidate the precise mechanisms of radiation-induced CNS injury, suggested mechanisms include oxidative stress, vascular injury and depletion of neural and glial progenitor cells. Radiotherapy has been shown to increase intracellular free radicals

within neurons following ionizing radiation, with animal models suggesting ongoing oxidative injury months after primary exposure (Tofilon & Fike, 2000). Other studies have highlighted the role of reactive inflammatory injury to the CNS microvasculature mediated by microglia (Monje et al., 2002; Monje et al., 2003; Mizumatsu et al., 2003). The vessel wall thickening and endothelial necrosis that are the hallmarks of radiation-induced CNS damage may globally disrupt cerebral blood flow, with particular consequences for dividing progenitor cell populations, which are intimately associated with and dependent on supplying microvascular structures (Dietrich et al., 2008).

Imaging chemotherapy-associated neurotoxicity

Voxel-based morphometry studies: Recent studies have investigated the effects of chemotherapy on global and regional brain volumes in breast cancer patients receiving chemotherapy using voxel-based morphometry, an MRI-based approach that segments the brains component tissues for volumetric analysis (Inagaki et al., 2007; McDonald et al., 2010; de Ruiters et al., 2012; Koppelmans et al., 2012; McDonald 2012; Hosseini 2012; for review see Kaiser et al., 2014, Simo et al., 2013). While the design and results of these studies are heterogeneous, they collectively support the notion of CNS toxicity associated with cancer therapy even for non-CNS malignancies, with measurable gray and white matter (WM) loss throughout the brain following standard treatment courses. Regional gray matter (GM) losses have been reported in numerous brain structures relevant to higher order cognition and executive function, including the prefrontal cortex, cingulate cortex, and medial temporal lobes (Inagaki et al., 2007; McDonald et al., 2010; de Ruiter et al., 2012). A recent study using graph theory to assess changes in structural connectivity revealed reduced clustering and small world indices in

fronto-temporal regions (Hosseini et al., 2012). Despite the burgeoning interest in this area, however, few studies have explored the longitudinal time course of these structural changed. With the exception of one prospective study with imaging at three time points over one year, these cross-sectional studies all depend on case-control comparisons to assay changes in brain anatomy between breast cancer patients and healthy controls, and therefore do not assess within-subject anatomical changes longitudinally.

Diffusion tensor imaging studies: Markers of neurotoxicity have also been explored using diffusion tensor imaging (DTI), an MRI-based method that measures the directional flow of water molecules to assess changes in WM integrity. Two commonly used DTI indices are the apparent diffusion coefficient (ADC) and fractional anisotropy (FA). ADC measures the magnitude of water diffusion in tissue, and is inversely proportional to the impedance of diffusion by intact cell membranes and myelin. Thus, ADC increases with loss of WM integrity. FA is a scalar value between 0 and 1 that indexes the directional uniformity of water diffusion, decreasing with loss of WM integrity.

As with VBM, DTI studies of chemotherapy-related brain changes have predominantly been conducted in the breast cancer population (Abraham et al., 2008; Deprez et al., 2011; Deprez et al., 2012; de Ruiter et al., 2012). Three of these studies were case-control designs, with average post-treatment follow-up ranging from 6 months to 9 years (Abraham et al., 2008; Deprez et al., 2011; de Ruiter et al., 2012). These studies consistently identified widespread decreases in WM integrity among post-chemotherapy breast cancer patients. WM changes in corpus callosum (Abraham et al., 2008) and frontal and temporal WM tracts (Deprez et al., 2011) were predictive of impairments in attention and psychomotor processing. Only one study (Deprez et al., 2012) assessed patients longitudinally, comparing 16 chemotherapy-exposed to 19

chemotherapy-naïve early stage breast cancer patients at baseline and 3-4 months following treatment. This study revealed significant post-treatment white matter changes scaling with decreased performance on tests of attention and verbal memory within chemotherapy-exposed patients.

Imaging radiation-associated neurotoxicity

Diffusion tensor imaging studies: While no VBM results on radiation-associated neuroanatomical changes have been reported, a handful of DTI studies have been published in recent years assessing the relationship between radiation therapy (RT), WM integrity and cognitive outcomes in patients receiving whole-brain RT. Three longitudinal studies have examined WM response to RT in patients with CNS neoplasms before, during and after whole brain RT (Nagesh et al., 2008; Nazem-Zadeh et al., 2012; Chapman et al., 2013). Dose-dependent demyelination has been observed in high-dose regions three months after completing focal RT, with dose-independent demyelination and axonal degeneration occurring 4-6 months after treatment (Nagesh et al., 2008). Two studies have highlighted the particular vulnerability of limbic structures, including the fornix and cingulate, and corpus callosum, with FA decreases as great as 50% between pre-RT and end-RT scans (Nazem-Zadeh et al., 2012; Chapman et al., 2013). A small number of case-control studies in survivors of childhood malignancy (Khong et al., 2006; Qiu et al., 2007; Dellani et al., 2008) demonstrated disseminated FA reductions in frontal, temporal, and parietal cortices, with WM abnormalities persisting into adulthood (Dellani et al., 2008).

The present study: rationale and significance

To our knowledge, no published studies have assessed longitudinal changes in brain structure in glioblastoma patients receiving combined systemic chemotherapy and cranial focal fractionated RT. Moreover, only a few studies in either the chemotherapy or radiation literature have assessed neuroradiographic parameters at multiple time points throughout the treatment protocol and with distant follow-up. Understanding the nature, severity and time course of neurotoxic injury at the level of neuroimaging is critically important for clarifying the relationship between the well-known clinical sequelae and the increasing body of preclinical studies on neurotoxicity associated with cancer therapy. Beyond adding to basic knowledge, understanding the effects of chemotherapy and RT on brain tissue will be an essential step in assessing the value of neuro-protective strategies. We were particularly interested in evaluating treatment-associated changes in brain regions critically important for endogenous neural repair and brain plasticity. Numerous studies have demonstrated toxicity to neural progenitor cells associated with exposure to chemotherapy and radiation (Monje et al., 2003; Dietrich et al, 2006). Specifically, the hippocampal dentate gyrus and the subventricular zone (SVZ) are known to supply neural and glial progenitor cells essential for adult neurogenesis, gliogenesis, cellular remodeling and neural repair. Injury to these cell populations may underlie the neurocognitive deficits and various other neurotoxic syndromes that have been observed among cancer survivors.

In the present study, we longitudinally examined the combined effects of chemotherapy and RT on radiographically tumor-free brain tissue in glioblastoma patients receiving temozolomide chemotherapy and focal fractionated RT, the current standard of care in newly diagnosed glioblastoma. We used voxel-wise tissue segmentation and diffusion tensor imaging to investigate longitudinal changes in tissue volumes and WM integrity over up to 9 months of

treatment. We examined volumetric changes at the whole brain (WB) level and within regions of interest (ROIs) encapsulating GM, WM, lateral ventricles and hippocampus. In addition, we used DTI to assess changes in WM integrity at the WB level and within ROIs sampling the SVZ.

A report of our findings is currently under review for publication (Prust et al., in submission).

Methods

Subjects and Treatment Protocol

Data were obtained through a prospective clinical study of glioblastoma patients conducted at our institution (NCT00756106). The local Institutional Review Board approved this protocol. All subjects provided written informed consent. The protocol employed serial MRI scans in patients receiving standard chemoradiation for glioblastoma after craniotomy for tumor resection. No additional investigational agents were allowed. Subjects received temozolomide (TMZ) at a daily oral dose of 75mg/m^2 concurrent with daily RT. RT was administered to the tumor core with a 1-2cm margin in thirty consecutive fractions of 2 Gy daily for a total dose of 60 Gy. One month after completing RT, patients underwent up to 12 cycles of TMZ at 150-200mg/m^2 daily on 5 consecutive days of a 28-day cycle.

Image acquisition

All MRI and DTI scans were acquired on a 3.0T MRI system (TimTrio, Siemens Medical Solutions, Malvern, PA). Patients were scanned twice before starting chemoradiation (3-7 days before and 1 day before), weekly during chemoradiation. and then monthly for six months. The MRI scanning protocol included pre- and post-contrast 1 mm^3 T1-weighted MEMPRAGE

images, fluid-attenuated inversion recovery (FLAIR) images, and diffusion tensor imaging (DTI).

Image processing

Five ROIs were outlined on the anatomical MRI images: normal appearing GM, normal appearing WM, anterior lateral ventricles, hippocampus and subventricular zone (**Figure 1**). Volumetric changes in non-tumor, normal-appearing brain tissue were assessed in GM, WM, lateral ventricles and hippocampus. In order to control for geometric distortions arising from changes in tumor morphology, GM and WM volumetric analyses were restricted to subjects in which tumor burden was confined to one hemisphere, with volumetric data being extracted from the tumor-free contralateral hemisphere. This was performed automatically by finding the mid-sagittal plane and comparing its position with respect to manually drawn tumor regions of interest (ROIs). We selected subjects that had at least five sequential imaging time points meeting this condition. MEMPRAGE images were de-noised using an algorithm based on a nonlocal means method (Jafari-Khouzani et al, 2014). Images were then segmented into WM, GM, and cerebrospinal fluid (CSF) using FSL (www.fmrib.ox.ac.uk/fsl). This was independently performed for each time point.

Lateral ventricle ROIs were constructed on T1-weighted MEMPRAGE images using semi-automatic tissue segmentation in ITK-SNAP (Yushkevich et al., 2006). ROIs were drawn on baseline images and non-rigidly co-registered using Advanced Normalization Tools (ANTs; Avants et al., 2011) to subsequent scans in each patient's imaging series. Ventricular ROIs were restricted to the anterior aspects of the lateral ventricles, given extensive posterior ventricular involvement in the majority of subjects that distorted ventricular anatomy and made assessment

of exclusively non-tumor related changes inaccurate (one subject was excluded due to excessive periventricular tumor involvement). The posterior margin of these ROIs was drawn at the point of maximum superior convexity of the overlying corpus callosum (**Figure 1**). Hippocampal ROIs were constructed on each subject's baseline MEMPRAGE images using manual tissue segmentation in ITK-SNAP based on a previously published protocol (Jafari-Khouzani et al, 2011) and non-rigidly co-registered to subsequent images using ANTs. This process allows ROIs drawn on baseline images to change with longitudinal alterations in tissue boundaries, and ROIs were visually inspected at each time point to ensure quality of fit. ROIs were drawn within the hemisphere of lowest tumor burden.

DTI parameters were examined in the hemisphere with lowest or no tumor burden. These parameters included the apparent diffusion coefficient (ADC) and fractional anisotropy (FA). ADC measures the magnitude of water diffusion in tissue, and is inversely proportional to the impedance of diffusion by intact cell membranes and myelin. FA is a scalar value between 0 and 1 that indexes the directional uniformity of water diffusion.

WM masks were generated by FSL from MEMPRAGE images at each time point. Since the resulting WM mask included some subcortical GM structures, they were identified and excluded by an atlas-based segmentation using the Harvard-Oxford atlas (Frazier et al, 2005; Makris et al., 2006; Desikan et al, 2006). Similarly, voxels occupied by tumor, or edema, were excluded from the WM mask using manually drawn tumor ROIs . For each subject, WM masks of all time points were registered into a common image space and their intersection was generated. The resulting WM mask was then re-registered to T2-weighted images at each time point.

ROI analysis was conducted within the lateral subventricular zone (SVZ) lining the lateral ventricles. This region was sampled with 5mm spherical ROIs centered within the WM supero-lateral to the ventricular wall within the hemisphere of lowest or no tumor burden on each patient's baseline scan (**Figure 1**). These ROIs were placed on the T2 MRI in the coronal plane at the anterior border of the lateral ventricle, and non-rigidly co-registered to the subsequent scans in each subject's series. ADC and FA maps were registered into the same T2 space, and values were extracted at each time point.

Data analysis

Voxel volumes were extracted from de-noised GM and WM masks and from co-registered ventricular masks at each time point using MATLAB (Natick, MA). Percentage change from baseline was plotted over time (**Figure 2**). Longitudinal volume changes were statistically assessed as a function of time (days) since the baseline scan using linear regression, controlling for patient age, gender and time-point specific tumor volume on FLAIR. For subjects remaining on the protocol up to or beyond the twelfth scanning session (23 weeks from baseline; N=6), pair-wise t-tests were conducted to compare ventricular volumes and WM ADC values at baseline and 23 weeks. This time point was chosen to capture sufficient time from baseline while avoiding prohibitive patient attrition at later time points.

Results

Patient characteristics

A total of 14 patients were analyzed (8 female, 6 male; mean age 60 (range 35-70); mean Karnofsky performance score 90 (range 60-100)). Following subtotal resection (N=10) or biopsy

(N=4), all patients completed 6 weeks of chemoradiation. During chemoradiation, 3 patients received no steroids, 7 patients were tapered off or continued on low dose steroids, and 4 patients required increased steroid dosing. Three subjects completed the full 35-week protocol. Attrition among the remaining 11 subjects was due to patient death, clinical decline, dose-limiting drug toxicities, or enrollment in an alternate therapeutic clinical trial.

VBM of WB, GM and WM volumes

Six subjects were excluded from WB, GM, and WM volume analysis, because they lacked five sequential imaging time points with unilateral tumor burden, a requirement of our automated tissue segmentation protocol. In the remaining 8 subjects, sample sizes at each time point were as follows: 8 at weeks 0 through 4, 7 at weeks 5 and 6, 5 at week 7, 8 at week 11, 6 at weeks 15 and 19, 4 on week 23, 3 at weeks 27, 31, and 35 (**Figure 2A-C**). WB volume decreased significantly ($F = 2.41$; $p = 0.016$; **Figure 2A**) from baseline to last follow-up, independent of age, gender and tumor volume. Cortical GM volumes also decreased during treatment ($F = 2.12$; $p = 0.036$; **Figure 2B**) independent of age, gender and tumor volume. WM volumes did not change significantly during treatment ($F = 0.70$; $p = 0.49$; **Figure 2C**). Representative structural differences before and after treatment are shown in **Figure 3**.

Volumetric analysis of anterior lateral ventricles and hippocampus

One subject was excluded from ventricular volumetric analysis due to extensive ventricular tumor involvement. Sample sizes at each time point in ventricular volume analysis were as follows: 13 at week 0, 11 at week 1, 12 at week 2, 11 and weeks 3 and 4, 12 and weeks 5 and 6, 10 at week 7, 11 at week 11, 10 and week 15, 8 at week 19, 6 at week 23, 5 at week 27, 2 at weeks 31 and 35. Significant anterior ventricular volume expansion was evident over time, independent of

age, gender, residual tumor volume, or steroid exposure during chemoradiation ($F = 15.247$; $p < 0.001$; **Figure 4A**). In subjects continuing on monthly temozolomide beyond 23 weeks (N=6), mean anterior lateral ventricle volume increased by 42.2% (SE: 8.8%; $t = 4.94$; $p < 0.005$; **Figure 4B**). In addition to these quantitative measures, ventricular dilatation was radiographically evident in most subjects (Supplemental Video e1). Hippocampal volumes showed no significant change over time (N=14; data not shown).

Diffusion tensor imaging

Within normal-appearing hemispheric WM masks contralateral to greatest tumor burden, no changes were observed in FA or ADC during chemoradiation (data not shown). ADC was measured within the subventricular zone of each subject, with sample sizes varying between time points as follows: 14 at week 0, 11 at week 1, 14 at week 2, 12 at weeks 3 and 4, 13 at weeks 5 and 6, 12 at weeks 7 and 11, 8 at weeks 15 and 19, 6 at week 23, 5 at week 27, 2 at weeks 31 and 35. ADC increases were seen within SVZ ROIs, independent of age, gender and tumor FLAIR volume ($F = 7.028$; $p < 0.001$; **Figure 5**). FA values within the lateral SVZ, however, showed no significant change over time (data not shown).

Discussion

We present longitudinal MRI-based evidence of tumor-independent structural brain changes in glioblastoma patients during combined treatment with systemic temozolomide and focal fractionated cranial RT. Progressive brain atrophy was observed through significant losses of WB volume, GM volume, dilatation of the lateral ventricles, and loss of WM integrity in the SVZ, with relative sparing of hippocampal volume and parenchymal WM. The use of serial

neuroimaging across multiple time points over several months offers a novel view of the nature, severity and long term time course of treatment-associated brain changes in glioma patients, and suggests that iatrogenic brain atrophy during anti-cancer treatment for intracranial neoplasms is both common and significant.

Ventricular dilatation following chemoradiation has been observed previously on longitudinal CT and MRI studies on chemoradiation for CNS neoplasms (Stylopoulos et al., 1988; Omuro et al., 2005). Notably, in one series (Stylopoulous et al., 1988), longitudinal ventricular enlargement scaled closely with progressive cortical atrophy, consistent with our findings of GM-predominant volume loss. In this way, ventricular dilatation appears to be a correlate of GM loss, and may prove to be a useful biomarker of longitudinal atrophy in the clinical setting. The association ventricular dilatation and GM loss has been observed in patients with dementia, with progressive ventricular dilatation predicting GM loss in cognitively relevant cortical surfaces (Madsen et al., 2015). It is plausible, therefore, that GM atrophy accounts for the observed expansion of CSF space, and that these changes may have consequences for neurocognitive function in patients receiving chemoradiation.

Surprisingly, we did not observe significant WM atrophy or DTI changes at the hemisphere level, despite the findings of prior studies that have documented WM volume loss, gliosis and demyelination in patients undergoing chemoradiation (Omuro et al., 2005; Simo et al., 2013; Kaiser et al., 2014). It is possible that focal, rather than whole-brain RT may spare parenchymal WM the atrophic changes that have been observed in other studies, and that the extent of WM damage within our dataset did not rise to the level of detectability within the hemispheric WM contralateral to the region of highest radiation exposure. Furthermore, we were limited by a relatively small sample size, and therefore our analysis may have been insufficiently

powered to detect subtle effects of neurotoxicity on parenchymal WM volume and DTI paramters.

Despite the absence of hemisphere-level WM changes, we did observe significant and progressive increases in ADC values within the SVZ, suggesting an accrued loss of WM integrity within this region over the treatment course. The SVZ is a dynamic and highly vascular region that is densely populated with NPCs, which are known to be vulnerable to irradiation (Monje et al., 2002) and multiple chemotherapeutic agents, even at subtherapeutic levels (Dietrich et al., 2006; Han et al., 2008). While it is impossible to attribute the observed ADC elevation to a specific etiology based on neuroimaging alone, it is reasonable to speculate that injury to the SVZ's dividing cell populations and microvasculature disrupts local diffusion properties. Given our limited sample size, this finding merits further observation in independent neuroimaging datasets, as well as histopathologic evaluation in post mortem human brain. To the extent that DTI changes in this region reflect meaningful cellular changes with implications for neurogenesis and gliogenesis, this finding could represent a useful biomarker to non-invasively assay ongoing injury to important stem cell populations. As neuroprotective strategies evolve in the coming years, such biomarkers can play a useful role in assessing the therapeutic benefit of efforts to spare sensitive regions from iatrogenic injury.

Atrophic brain changes followed a delayed time course, with minimal changes seen within the first six weeks of treatment, after which WB and GM volume loss and ventricular dilatation appeared to follow a progressive pattern for the remainder of the observation period. Our data do not, however, provide conclusive evidence regarding the long-term durability or potential reversibility of these changes, as attrition to disease progression or death caused significant subject attrition after 23 weeks, with the longest follow up being 35 weeks from

baseline imaging. While we did not find evidence of reversibility within this time period, we cannot exclude the possibility that some degree of CNS repair leads to partial or complete reversal of morphometric changes in long-term survivors. Exploration of this question awaits further studies with years, rather than months, of longitudinal evaluation, and may require study in patients with lower-grade intracranial neoplasms with longer average survival periods.

Interestingly, the onset of significant morphologic changes appears to coincide with the time of RT completion, with relative stability of volumteric and DTI parameters during the six weeks of chemoradiation. Given the concurrent administration of chemotherapy and RT, we were unable in the present study to parse the independent effects of these two treatment modalities, or to assess whether they interact with one another to produce neurotoxic effects out of proportion to the main effects of either one alone. Preclinical studies suggest that combined chemoradiation yields synergistic toxic effects (Monje et al., 2002) and patients treated with chemoradiation appear to experience greater memory, attention and executive function deficits compared to those undergoing chemotherapy alone (Correa et al., 2012). It is possible that radiation represents the predominant driver of these changes, with early exposure initiating a neurodegenerative process that progresses over time even in the absence of ongoing exposure radiation exposure. It is also conceivable, however, that progressive brain changes result from the synergistic effects of chemotherapy *and* radiation, and that ongoing monthly chemotherapy after completion of RT is an important driver of brain atrophy. Additionally, novel targeted therapies, such as anti-angiogenic agents are entering mainstream clinical practice, with unknown effects on healthy brain tissue. Large datasets investigating exposure to anti-angiogenic agents (Batchelor et al., 2013) and separate use of chemotherapy and radiation (Wick et al., 2012) are

emerging, and will be indispensable to future investigations of neurotoxicity from cancer therapies.

Though our findings provide strong evidence of structural brain changes that suggest a real neuroanatomic phenotype, our cohort's small size, particularly after subject attrition at later time points, limits the generalizability of our findings and merits caution in their interpretation. Definitive confirmation and validation of our findings must await further exploration in larger datasets. Beyond issues pertaining to sample size and inability to separately investigate the effects of chemotherapy and RT, our study was limited by the absence of detailed cognitive performance measures to correlate with the observed structural changes on neuroimaging. Because these data were collected as part of trial whose stated purpose was to investigate the effects of treatment on tumor volume, rather than on healthy brain tissue, neurocognitive parameters were not a initially a focus of investigation. Other measures of performance status, such as the Karnofsky performance status, mini-mental state exam, and chart review of patient's clinical status at each visit proved insufficiently sensitive for correlation with our neuroimaging findings. Given the extent of cerebral atrophy, however, and the well-documented effects of anti-cancer therapy on multiple domains of cognitive performance, it will be essential to investigate the relationship between brain atrophy and neurocognitive changes in future studies.

In order to correlate neurocognitive outcomes with structural brain changes, longitudinal prospective trials are needed to examine performance in multiple cognitive domains in concert with serial neuroimaging. Such data will help characterize the functional effects of structural brain changes within this population, and may also clarify the significance of individual differences in brain volume loss. For example, it is conceivable that rapid early volume loss

might be a sensitive indicator of worse neurocognitive outcome, and prediction models based on such individual differences may help stratify risk for long-term adverse effects.

It should further be noted that imaging analysis in brain tumor patients remains challenging. Our analyses were constrained by the presence of a dynamically changing tumor burden with considerable mass effect and visit-to-visit variability in tumor size and surrounding edema. Given our relatively small sample size and the frequency of bilateral tumor burden in our subjects, we were unable to restrict many of our analyses to patients with a tumor-free hemisphere. Therefore, we included data from manually drawn ROIs when tumor burden did not appear to involve the structure of interest; however, future studies in brain cancer patients undergoing combined chemoradiation may preferentially include patients with minimal tumor burden, or who have undergone a gross total tumor resection to further validate the effects of chemoradiation on the normal brain.

Finally, it is not unreasonable to question the relevance of our findings in terms of management of patients with high-grade CNS malignancy, whose expected survival is on the order of months. Chemotherapy and radiation are essential life-extending interventions, and we do not take the position that their use should be curtailed to avoid neurotoxic side effects. We would argue, however, that exploring these effects in glioblastoma patients is important for three reasons. First, glioblastoma is not the only malignancy that is treated with combined chemotherapy and cranial RT. Lower grade tumors, such as primary CNS lymphoma, are treated with similar regimens, and our dataset provides a model of neurotoxic changes that may be extrapolated to clinical populations with longer expected survival. Systemic chemotherapy and whole-brain RT are also used for various non-CNS neoplasms, including lung cancer, breast cancer and hematologic malignancies, and our findings may offer insight into treatment-associated neurologic changes within these populations as well. Second, efforts to limit

neurotoxic exposure, either through radiation planning that maximally spares non-tumor brain tissue or through neuroprotective pharmacotherapy (Weitzel et al., 2015) are currently underway. While glioblastoma is characterized by notoriously short survival, patients may live for months or even years with progression-free disease, and minimizing treatment-associated toxicity to optimize quality of life is an important clinical priority. Finally, it is conceivable that innovations in medical, surgical and radiation therapy may prolong survival for these patients in the years to come, and understanding how early exposure to therapy affects long-term neurologic health may guide future neuroprotective efforts.

As novel therapies have improved cancer survival, the delayed effects of treatment-associated toxicity in survivors represent a particular challenge for oncologists and neurologists seeking to maximize patients' quality of life. Characterizing imaging biomarkers and the natural history of neurologic injury secondary to chemotherapy and radiation is essential not only for optimal clinical management of cancer patients, but as a foundation for developing and testing neuroprotective strategies.

References

Abraham J, Haut MW, Moran MT, Filburn S, Lemiuex S, Kuwabara H. Adjuvant chemotherapy for breast cancer: effects on cerebral white matter seen in diffusion tensor imaging. Clin Breast Cancer. 2008 Feb;8(1):88–91.

Ahles TA, Saykin AJ, Furstenberg CT, Cole B, Mott LA, Skalla K, et al. Neuropsychologic impact of standard-dose systemic chemotherapy in long-term survivors of breast cancer and lymphoma. J Clin Oncol. 2002 Jan 15;20(2):485–93.

Avants BB, Tustison NJ, Song G, Cook PA, Klein A, Gee JC. A reproducible evaluation of ANTs similarity metric performance in brain image registration. Neuroimage. 2011 Feb 1;54(3):2033–44.

Batchelor TT, Gerstner ER, Emblem KE, Duda DG, Kalpathy-Cramer J, Snuderl M, et al. Improved tumor oxygenation and survival in glioblastoma patients who show increased blood perfusion after cediranib and chemoradiation. Proc Natl Acad Sci U S A. 2013 Nov 19;110(47):19059–64

Chang A, Nishiyama A, Peterson J, Prineas J, Trapp BD. NG2-positive oligodendrocyte progenitor cells in adult human brain and multiple sclerosis lesions. J Neurosci. 2000 Sep 1;20(17):6404–12.

Chapman CH, Nazem-Zadeh M, Lee OE, Schipper MJ, Tsien CI, Lawrence TS, et al. Regional variation in brain white matter diffusion index changes following chemoradiotherapy: a prospective study using tract-based spatial statistics. PLoS One. 2013 Jan;8(3):e57768.

Correa DD, Shi W, Abrey LE, Deangelis LM, Omuro AM, Deutsch MB, et al. Cognitive functions in primary CNS lymphoma after single or combined modality regimens. Neuro Oncol. 2012 Jan;14(1):101–8.

Curtis MA, Faull RLM, Eriksson PS. The effect of neurodegenerative diseases on the subventricular zone. Nat Rev Neurosci. 2007 Sep;8(9):712–23.

de Ruiter MB, Reneman L, Boogerd W, Veltman DJ, Caan M, Douaud G, et al. Late effects of high-dose adjuvant chemotherapy on white and gray matter in breast cancer survivors: converging results from multimodal magnetic resonance imaging. Hum Brain Mapp. 2012 Dec;33(12):2971–83.

Dellani PR, Eder S, Gawehn J, Vucurevic G, Fellgiebel A, Müller MJ, et al. Late structural alterations of cerebral white matter in long-term survivors of childhood leukemia. J Magn Reson Imaging. 2008 Jun;27(6):1250–5.

Deng W, Aimone JB, Gage FH. New neurons and new memories: how does adult hippocampal neurogenesis affect learning and memory? Nat Rev Neurosci. 2010 May;11(5):339–50.

Deprez S, Amant F, Smeets A, Peeters R, Leemans A, Van Hecke W, et al. Longitudinal assessment of chemotherapy-induced structural changes in cerebral white matter and its correlation with impaired cognitive functioning. J Clin Oncol. 2012 Jan 20;30(3):274–81.

Deprez S, Amant F, Yigit R, Porke K, Verhoeven J, Van den Stock J, et al. Chemotherapy-induced structural changes in cerebral white matter and its correlation with impaired cognitive functioning in breast cancer patients. Hum Brain Mapp. 2011 Mar;32(3):480–93.

Desikan RS, Ségonne F, Fischl B, Quinn BT, Dickerson BC, Blacker D, et al. An automated labeling system for subdividing the human cerebral cortex on MRI scans into gyral based regions of interest. Neuroimage. 2006 Jul 1;31(3):968–80.

Dietrich J, Han R, Yang Y, Mayer-Pröschel M, Noble M. CNS progenitor cells and oligodendrocytes are targets of chemotherapeutic agents in vitro and in vivo. J Biol. 2006 Jan;5(7):22.

Dietrich J, Monje M, Wefel J, Meyers C. Clinical patterns and biological correlates of cognitive dysfunction associated with cancer therapy. Oncologist. 2008 Dec;13(12):1285–95.

Eriksson PS, Perfilieva E, Björk-Eriksson T, Alborn AM, Nordborg C, Peterson DA, et al. Neurogenesis in the adult human hippocampus. Nat Med. 1998 Nov;4(11):1313–7.

Frazier JA, Chiu S, Breeze JL, Makris N, Lange N, Kennedy DN, et al. Structural brain magnetic resonance imaging of limbic and thalamic volumes in pediatric bipolar disorder. Am J Psychiatry. 2005 Jul;162(7):1256–65.

Han R, Yang YM, Dietrich J, Luebke A, Mayer-Pröschel M, Noble M. Systemic 5-fluorouracil treatment causes a syndrome of delayed myelin destruction in the central nervous system. J Biol. 2008 Jan;7(4):12.

Hosseini SMH, Koovakkattu D, Kesler SR. Altered small-world properties of gray matter networks in breast cancer. BMC Neurol. 2012 Jan;12:28.

Inagaki M, Yoshikawa E, Matsuoka Y, Sugawara Y, Nakano T, Akechi T, et al. Smaller regional volumes of brain gray and white matter demonstrated in breast cancer survivors exposed to adjuvant chemotherapy. Cancer. 2007 Jan 1;109(1):146–56.

Jafari-Khouzani K. MRI upsampling using feature-based nonlocal means approach. IEEE Trans Med Imaging. 2014 Oct;33(10):1969–85.

Jafari-Khouzani K, Elisevich K V, Patel S, Soltanian-Zadeh H. Dataset of magnetic resonance images of nonepileptic subjects and temporal lobe epilepsy patients for validation of hippocampal segmentation techniques. Neuroinformatics. 2011 Dec;9(4):335–46.

Kaiser J, Bledowski C, Dietrich J. Neural correlates of chemotherapy-related cognitive impairment. Cortex. 2014 May;54:33–50.

Kempermann G, Kuhn HG, Gage FH. More hippocampal neurons in adult mice living in an enriched environment. Nature. 1997 Apr 3;386(6624):493–5.

Kempermann G. The neurogenic reserve hypothesis: what is adult hippocampal neurogenesis good for? Trends Neurosci. 2008 Apr;31(4):163–9.

Khong P-L, Leung LHT, Fung ASM, Fong DYT, Qiu D, Kwong DLW, et al. White matter anisotropy in post-treatment childhood cancer survivors: preliminary evidence of association with neurocognitive function. J Clin Oncol. 2006 Feb 20;24(6):884–90.

Koppelmans V, de Ruiter MB, van der Lijn F, Boogerd W, Seynaeve C, van der Lugt A, et al. Global and focal brain volume in long-term breast cancer survivors exposed to adjuvant chemotherapy. Breast Cancer Res Treat. 2012 Apr;132(3):1099–106.

Koppelmans V, de Groot M, de Ruiter MB, Boogerd W, Seynaeve C, Vernooij MW, et al. Global and focal white matter integrity in breast cancer survivors 20 years after adjuvant chemotherapy. Hum Brain Mapp. 2014 Mar;35(3):889–99.

Lemaire V, Koehl M, Le Moal M, Abrous DN. Prenatal stress produces learning deficits associated with an inhibition of neurogenesis in the hippocampus. Proc Natl Acad Sci U S A. 2000 Sep 26;97(20):11032–7.

Madsen SK, Gutman BA, Joshi SH, Toga AW, Jack CR, Weiner MW, et al. Mapping ventricular expansion onto cortical gray matter in older adults. Neurobiol Aging. 2015 Jan;36 Suppl 1:S32–41.

McDonald BC, Conroy SK, Smith DJ, West JD, Saykin AJ. Frontal gray matter reduction after breast cancer chemotherapy and association with executive symptoms: a replication and extension study. Brain Behav Immun. 2013 Mar;30 Suppl:S117–25.

Mizumatsu S, Monje ML, Morhardt DR, Rola R, Palmer TD, Fike JR. Extreme sensitivity of adult neurogenesis to low doses of X-irradiation. Cancer Res. 2003 Jul 15;63(14):4021–7.

Monje ML, Mizumatsu S, Fike JR, Palmer TD. Irradiation induces neural precursor-cell dysfunction. Nat Med. 2002 Sep;8(9):955–62.

Monje ML, Toda H, Palmer TD. Inflammatory blockade restores adult hippocampal neurogenesis. Science. 2003 Dec 5;302(5651):1760–5.

Monje M, Dietrich J. Cognitive side effects of cancer therapy demonstrate a functional role for adult neurogenesis. Behav Brain Res. 2012 Feb 14;227(2):376–9.

Nagesh V, Tsien CI, Chenevert TL, Ross BD, Lawrence TS, Junick L, et al. Radiation-induced changes in normal-appearing white matter in patients with cerebral tumors: a diffusion tensor imaging study. Int J Radiat Oncol Biol Phys. 2008 Mar 15;70(4):1002–10.

Nazem-Zadeh M-R, Chapman CH, Lawrence TL, Tsien CI, Cao Y. Radiation therapy effects on white matter fiber tracts of the limbic circuit. Med Phys. 2012 Sep;39(9):5603–13.

Omuro AMP, Ben-Porat LS, Panageas KS, Kim AK, Correa DD, Yahalom J, et al. Delayed neurotoxicity in primary central nervous system lymphoma. Arch Neurol. American Medical Association; 2005 Oct 1;62(10):1595–600.

Parihar VK, Limoli CL. Cranial irradiation compromises neuronal architecture in the hippocampus. Proc Natl Acad Sci U S A. 2013 Jul 30;110(31):12822–7.

Prust MJ, Jafari-Khouzani K, Kalpathy-Cramer J, Polaskova P, Batchelor TT, Gerstner EG, Dietrich J. Standard chemoradiation for glioblastoma results in progressive brain volume loss. Neurology. In submission.

Qiu D, Kwong DLW, Chan GCF, Leung LHT, Khong P-L. Diffusion tensor magnetic resonance imaging finding of discrepant fractional anisotropy between the frontal and parietal lobes after whole-brain irradiation in childhood medulloblastoma survivors: reflection of regional white matter radiosensitivity? Int J Radiat Oncol Biol Phys. 2007 Nov 1;69(3):846–51.

Schagen SB, van Dam FS, Muller MJ, Boogerd W, Lindeboom J, Bruning PF. Cognitive deficits after postoperative adjuvant chemotherapy for breast carcinoma. Cancer. 1999 Feb 1;85(3):640–50.

Simó M, Rifà-Ros X, Rodriguez-Fornells A, Bruna J. Chemobrain: a systematic review of structural and functional neuroimaging studies. Neurosci Biobehav Rev. 2013 Sep;37(8):1311–21.

Stylopoulos LA, George AE, de Leon MJ, Miller JD, Foo SH, Hiesiger E, et al. Longitudinal CT study of parenchymal brain changes in glioma survivors. AJNR Am J Neuroradiol. American Society of Neuroradiology; 1988 Jan 1;9(3):517–22.

Tada E, Parent JM, Lowenstein DH, Fike JR. X-irradiation causes a prolonged reduction in cell proliferation in the dentate gyrus of adult rats. Neuroscience. 2000 Jan;99(1):33–41.

Tanaka S, Louis DN, Curry WT, Batchelor TT, Dietrich J. Diagnostic and therapeutic avenues for glioblastoma: no longer a dead end? Nat Rev Clin Oncol. 2013 Jan;10(1):14–26.

Taphoorn MJB, Klein M. Cognitive deficits in adult patients with brain tumours. Lancet Neurol. 2004 Mar;3(3):159–68.

Tofilon PJ, Fike JR. The radioresponse of the central nervous system: a dynamic process. Radiat Res. 2000 Apr;153(4):357–70.

van Dam FS, Schagen SB, Muller MJ, Boogerd W, vd Wall E, Droogleever Fortuyn ME, et al. Impairment of cognitive function in women receiving adjuvant treatment for high-risk breast

cancer: high-dose versus standard-dose chemotherapy. J Natl Cancer Inst. 1998 Feb 4;90(3):210–8.

van Praag H, Christie BR, Sejnowski TJ, Gage FH. Running enhances neurogenesis, learning, and long-term potentiation in mice. Proc Natl Acad Sci U S A. 1999 Nov 9;96(23):13427–31.

Wefel JS, Lenzi R, Theriault RL, Davis RN, Meyers CA. The cognitive sequelae of standard-dose adjuvant chemotherapy in women with breast carcinoma: results of a prospective, randomized, longitudinal trial. Cancer. 2004 Jun 1;100(11):2292–9.

Weitzel DH, Tovmasyan A, Ashcraft KA, Rajic Z, Weitner T, Liu C, et al. Radioprotection of the Brain White Matter by Mn(III) N-Butoxyethylpyridylporphyrin-Based Superoxide Dismutase Mimic MnTnBuOE-2-PyP5+. Mol Cancer Ther. 2015 Jan;14(1):70–9.

Welzel T, Niethammer A, Mende U, Heiland S, Wenz F, Debus J, et al. Diffusion tensor imaging screening of radiation-induced changes in the white matter after prophylactic cranial irradiation of patients with small cell lung cancer: first results of a prospective study. AJNR Am J Neuroradiol. 2008 Feb;29(2):379–83.

Wick W, Platten M, Meisner C, Felsberg J, Tabatabai G, Simon M, et al. Temozolomide chemotherapy alone versus radiotherapy alone for malignant astrocytoma in the elderly: the NOA-08 randomised, phase 3 trial. Lancet Oncol. 2012 Jul;13(7):707–15.

Yushkevich PA, Piven J, Hazlett HC, Smith RG, Ho S, Gee JC, et al. User-guided 3D active contour segmentation of anatomical structures: significantly improved efficiency and reliability. Neuroimage. 2006 Jul 1;31(3):1116–28.

Zhao C, Deng W, Gage FH. Mechanisms and functional implications of adult neurogenesis. Cell. 2008 Feb 22;132(4):645–60.

Figures
Figure 1

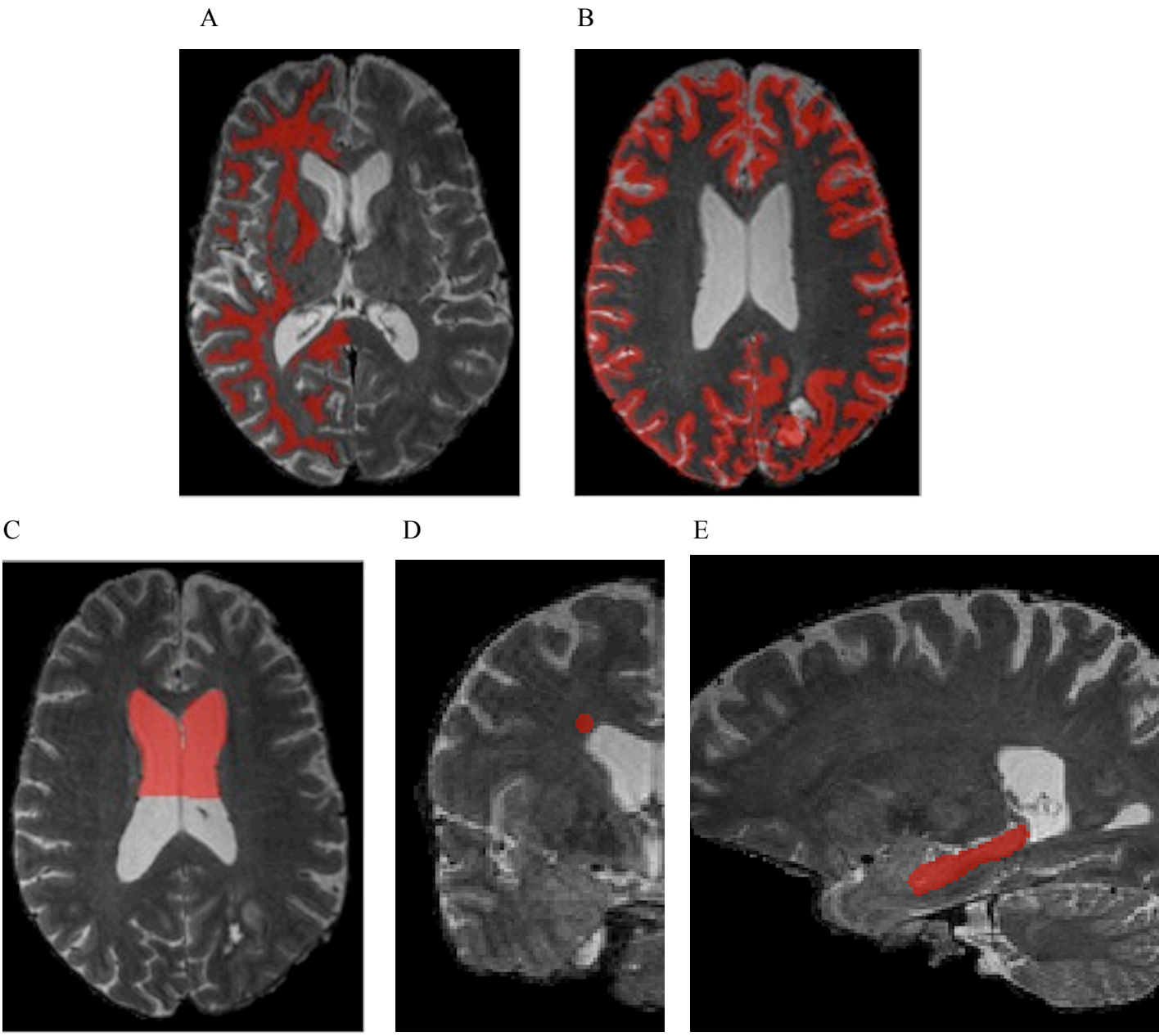

Figure 2

A

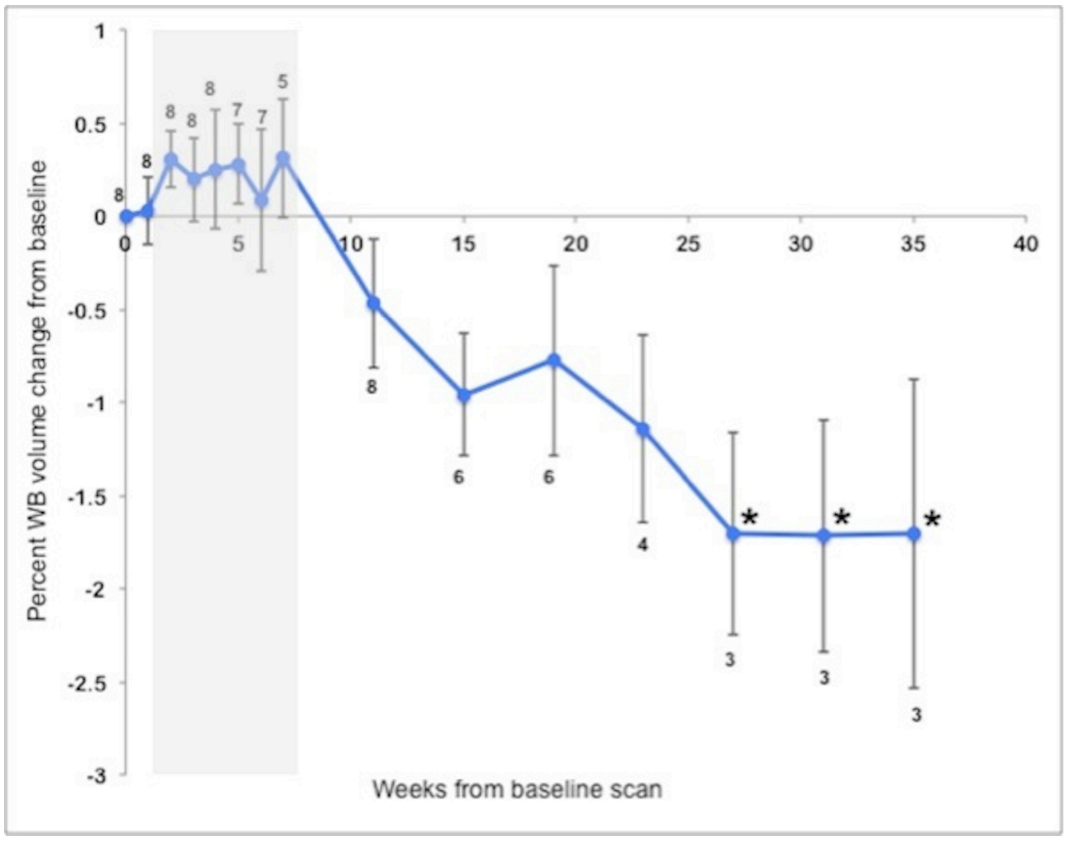
Percent WB volume change from baseline
Weeks from baseline scan
1
0.5
0
-0.5
-1
-1.5
-2
-2.5
-3
0
5
10
15
20
25
30
35
40
*
*
*

B

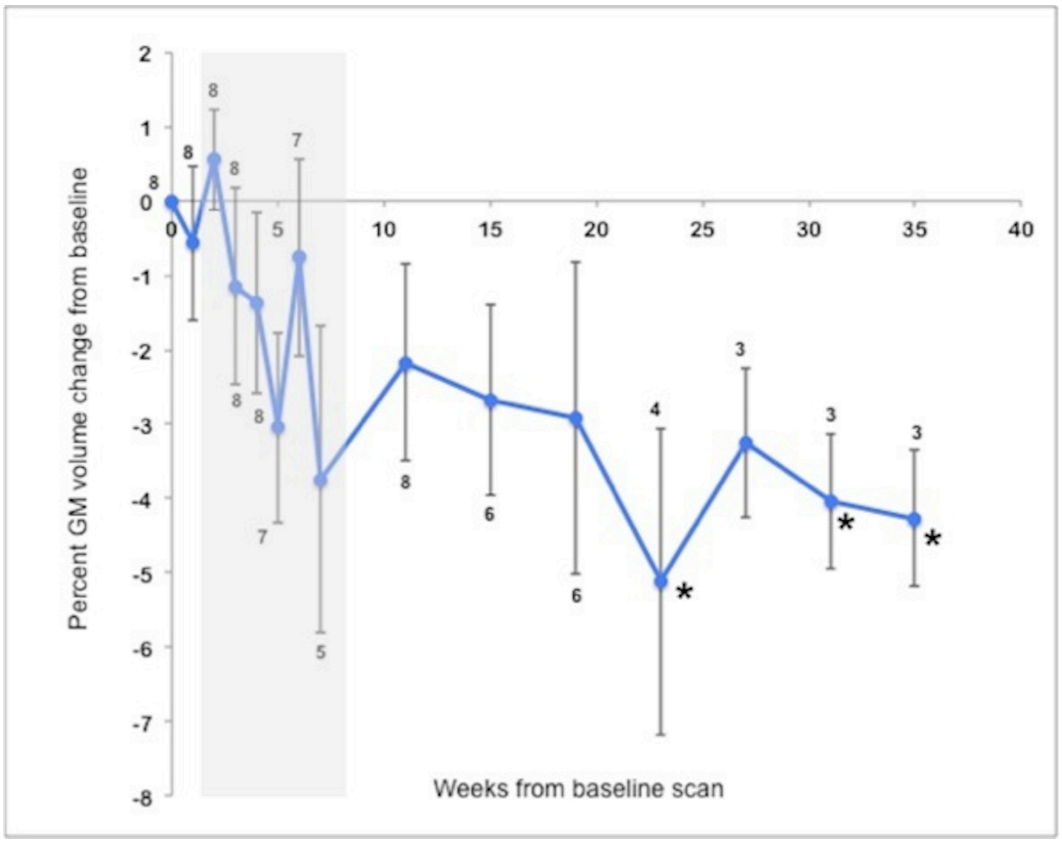
Percent GM volume change from baseline
Weeks from baseline scan
2
1
0
-1
-2
-3
-4
-5
-6
-7
-8
0
5
10
15
20
25
30
35
40
*
*
*

C

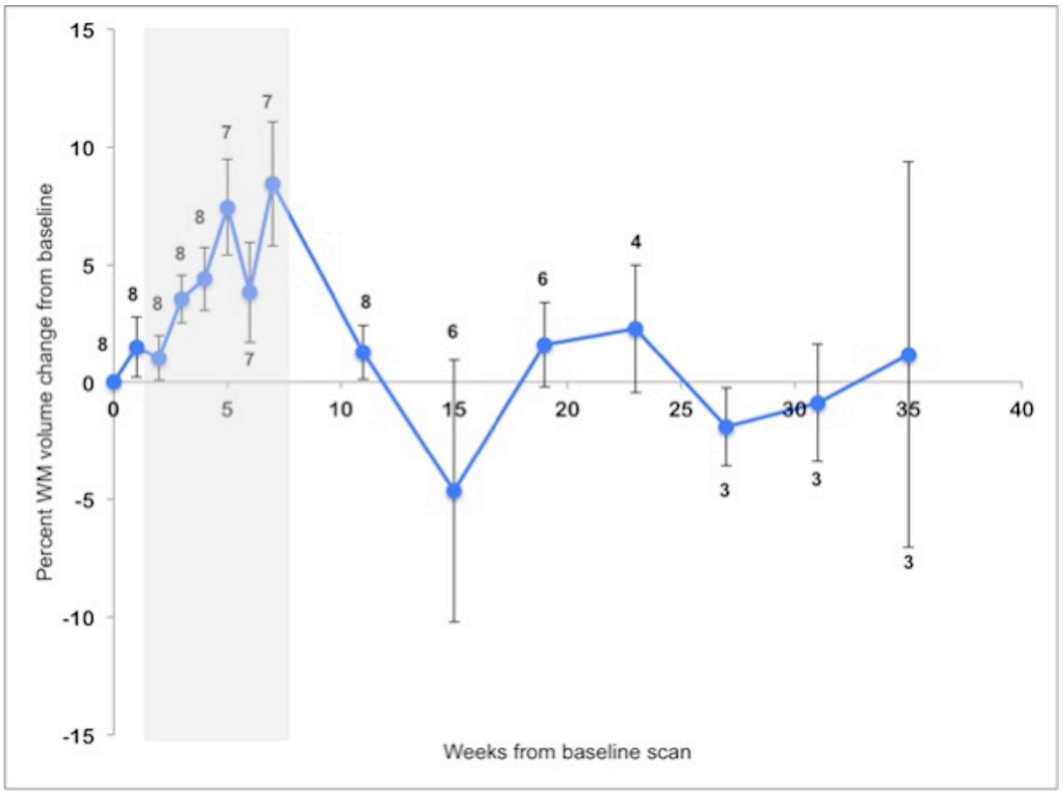
Percent WM volume change from baseline
Weeks from baseline scan
15
10
5
0
-5
-10
-15
0
5
10
15
20
25
30
35
40
8
8
8
8
7
7
8
6
6
4
3
3
3

Figure 3

A

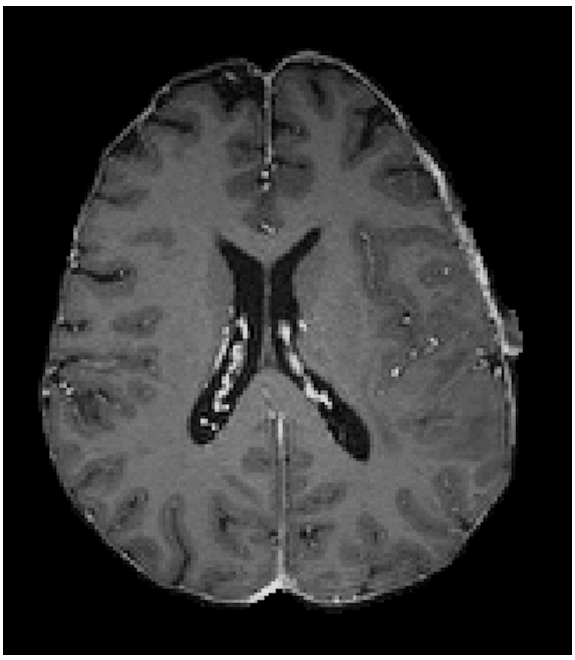

B

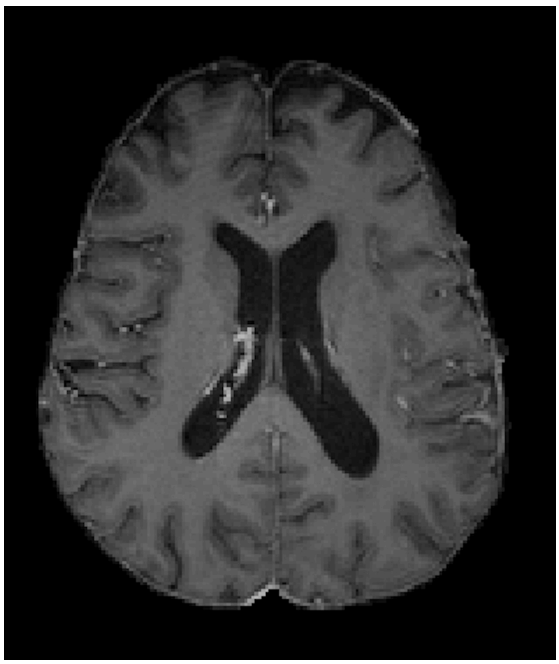

Figure 4

A

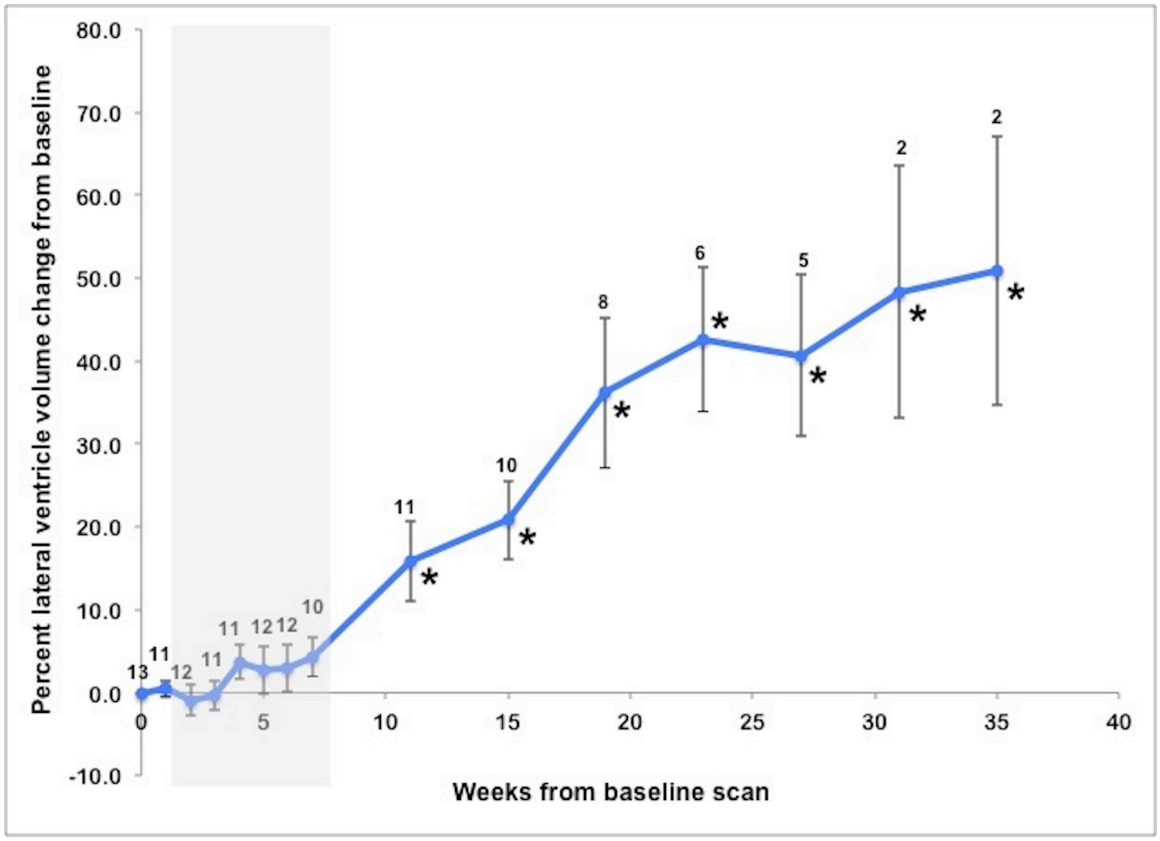
Percent lateral ventricle volume change from baseline
80.0
70.0
60.0
50.0
40.0
30.0
20.0
10.0
0.0
-10.0
0
5
10
15
20
25
30
35
40
Weeks from baseline scan
13
11
12
11
11
12
12
10
11
10
8
6
5
2
2
*

B

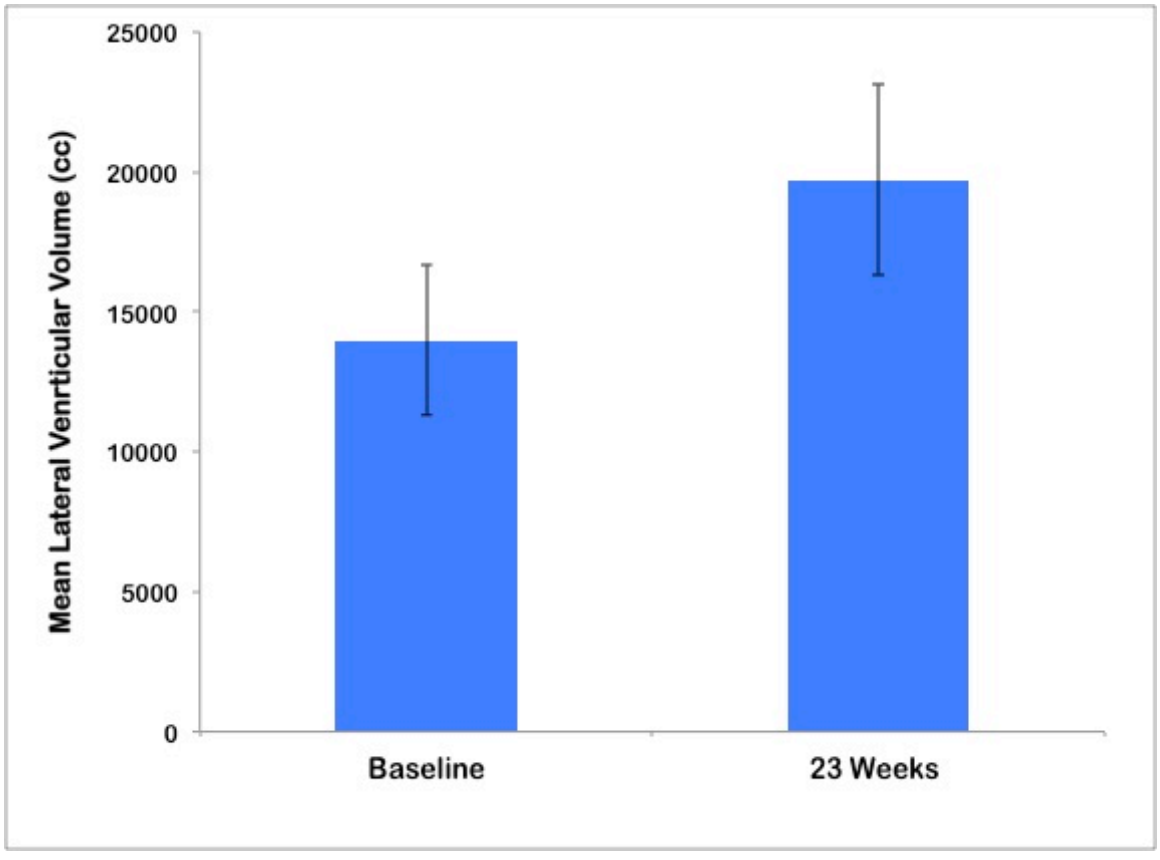
Mean Lateral Venrticular Volume (cc)
25000
20000
15000
10000
5000
0
Baseline
23 Weeks

Figure 5

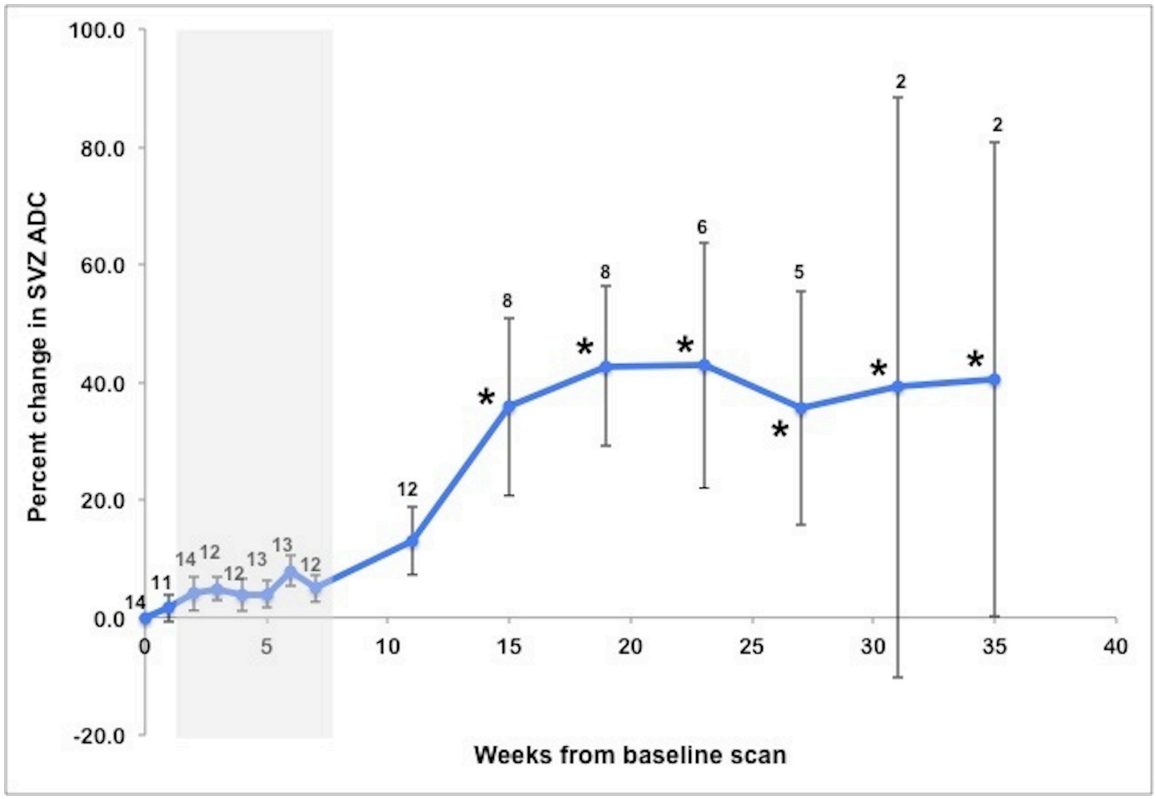
100.0
80.0
60.0
40.0
20.0
0.0
-20.0
Percent change in SVZ ADC
0
5
10
15
20
25
30
35
40
Weeks from baseline scan
14
11
14
12
12
13
13
12
12
8
8
6
5
2
2
*
*
*
*
*
*

Video 1

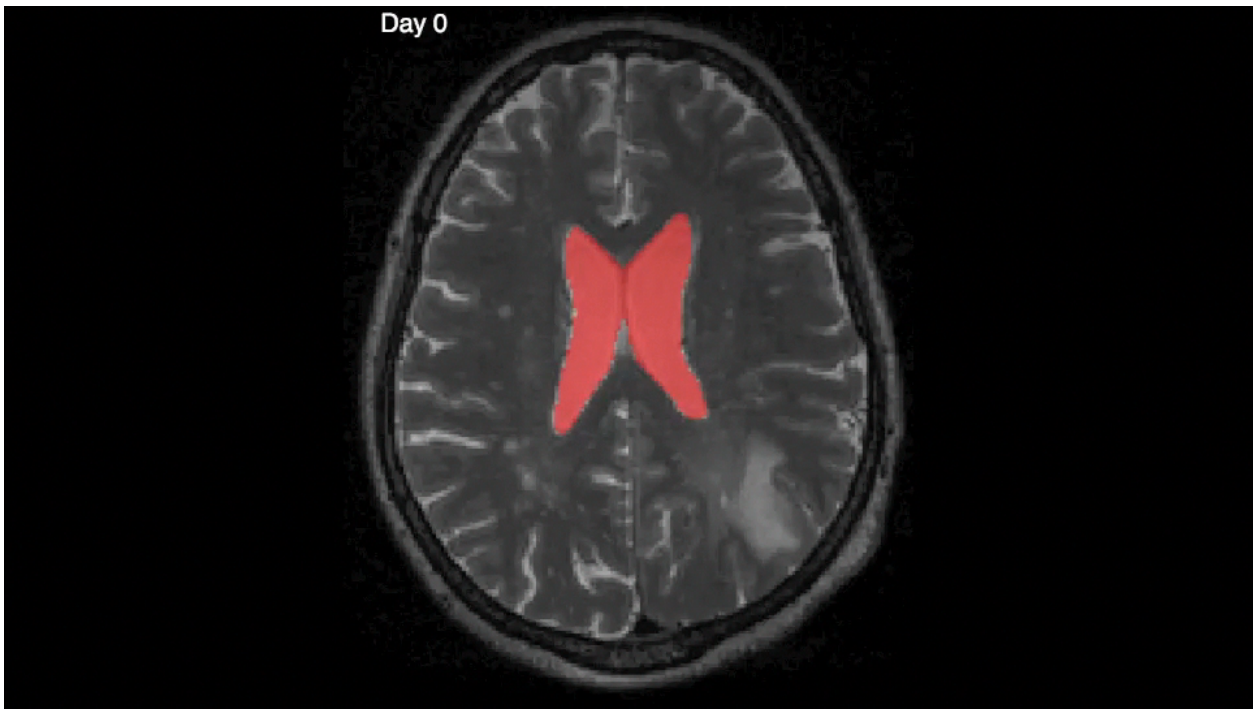

Figure Legends

Figure 1: Representative regions of interest for WM (A), GM (B), anterior lateral ventricle (C), SVZ (D) and hippocampus (E).

Figure 2: WB (A), GM (B), and WM (C) volumes across the treatment period. Data points represent the sample mean of percent volume change from baseline at each time point. Error bars represent the standard error of the mean. Sample sizes are indicated at each time point. Grey shading indicates combined chemotherapy and radiation. Six subjects did not meet criteria for volumetric analysis. *Indicates time points at which volumetric changes are statistically significant ($p < 0.05$).

Figure 3: Panel A – Pre-treatment baseline T1 scan. Panel B – Post-treatment T1 scan (28 weeks from baseline).

Figure 4: Panel A - Lateral ventricular volumes across the treatment period. Data points represent the sample mean of percent volume change from baseline at each time point. Error bars represent the standard error of the mean. Sample sizes are indicated at each time point. Grey shading indicates combined chemotherapy and radiation. One subject was excluded due to extensive ventricular tumor involvement. *Indicates time points at which volumetric changes are statistically significant ($p < 0.05$). Panel B – Lateral ventricular volumes at baseline and 23 weeks in subjects remaining on the protocol to this point (N=6). Bars represent sample means at baseline and 23 weeks, error bars represent the standard error of the mean.

Figure 5: ADC values from SVZ ROI across the treatment period. Data points represent the sample mean of percent volume change from baseline at each time point. Error bars represent the standard error of the mean. Sample sizes are indicated at each time point. Grey shading indicates combined chemotherapy and radiation. *Indicates time points at which volumetric changes are statistically significant ($p < 0.05$).

Video 1: Video displaying T2-weighted images from one subject at each time point. Red area represents the ventricular area from the patient's baseline scan. Days since baseline are displayed in the upper left corner.